Article

Insights into AT$_1$ Receptor Activation through AngII Binding Studies

Minos-Timotheos Matsoukas,[†] Constantinos Potamitis,[‡] Panayiotis Plotas,[§] Maria-Eleni Androutsou,[§] George Agelis,[§] John Matsoukas,*[,§] and Panagiotis Zoumpoulakis*[,‡]
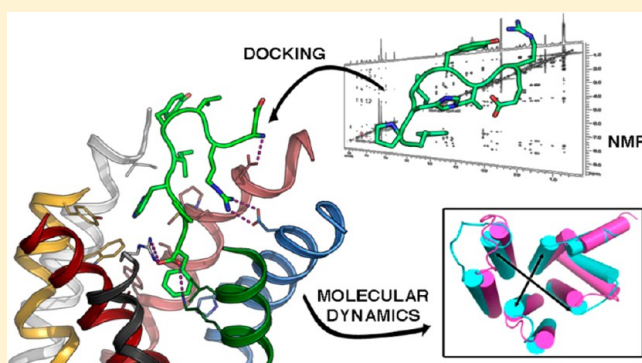
[†]Laboratori de Medicina Computacional, Unitat de Bioestadıstica, Facultat de Medicina, Universitat Autonoma de Barcelona, E-08193, Bellaterra, Barcelona, Spain

[‡]Institute of Biology, Medicinal Chemistry and Biotechnology, National Hellenic Research Foundation, 48, Vas. Constantinou Avenue, GR-11635, Athens, Greece

[§]Laboratory of Organic Chemistry, Biochemistry and Natural Products, Department of Chemistry, University of Patras, GR-26500, Rion, Patras, Greece

Ⓦ Web-Enhanced Feature   Ⓢ Supporting Information

ABSTRACT: This study investigates the binding of angiotensin II (AngII) to the angiotensin II type 1 receptor (AT$_1$R), taking into consideration several known activation elements that have been observed for G-protein-coupled receptors (GPCRs). In order to determine the crucial interactions of AngII upon binding, several MD simulations were implemented using AngII conformations derived from experimental data (NMR ROEs) and *in silico* flexible docking methodologies. An additional goal was to simulate the induced activation mechanism and examine the already known structural rearrangements of GPCRs upon activation. Performing MD simulations to the AT$_1$R − AngII − lipids complex, a series of dynamic changes in the topology of AngII and the intracellular part of the receptor were observed. Overall, the present study proposes a complete binding profile of AngII to the AT$_1$R, as well as the key transitional elements of the receptor and the agonist peptide upon activation through NMR and *in silico* studies.

INTRODUCTION

One of the major systems, which affects the regulation of blood pressure, thus plays an integral role in the pathophysiology of hypertension, is the Renin Angiotensin Aldosterone System (RAAS). The octapeptide hormone angiotensin II is the active product of RAAS, which causes vasoconstriction upon binding into the active site of the AT$_1$ receptor. This receptor is widespread in organs and tissues but is found predominately in vascular and myocardial tissue, the liver, the adrenal cortex, and some areas of the brain.[1,2] AngII not only mediates immediate physiological effects of vasoconstriction and blood pressure regulation but is also implicated in inflammation, endothelial dysfunction, atherosclerosis, and congestive heart failure. Furthermore, AngII causes aldosterone secretion and sympathetic activation, which again contribute to the development of hypertension.

The AT$_1$ receptor is a G-protein-coupled receptor. GPCRs constitute the largest group of membrane receptors, including receptors for angiotensin, epinephrine and norepinephrine, acetylcholine, adenosine, dopamine, endothelin, vasopressin, serotonin, and many other hormones and neurotransmitters. Recent advances in GPCR crystallography have resulted in a vast growth of the number of solved structures, including the structure of the fully active state of the β_2 adrenergic receptor in complex with the G protein[3] and the agonist bound states of the A$_{2A}$ adenosine[4] and neurotensin[5] receptors. These findings have since assisted the exploration of activation mechanisms of other GPCRs through homology modeling.

AT$_1$ receptor activation follows similar signaling mechanisms with GPCRs, involving the activation of adenyl-cyclase, phosphatase, and kinase, as well as changes in intracellular calcium. AT$_1$R mainly activates the heterotrimeric G$_{q/11}$ protein of the G protein family and phospholipase C pathway to produce second messengers, such as inositol trisphosphate (IP3) and diacylglycerol (DAG), which mobilize the intracellular calcium stores and activate protein kinases C, respectively. Other G protein-dependent or -independent signaling pathways are also activated by the AT$_1$ receptor.[6]

As many other GPCRs, the AT$_1$ receptor exists in different conformational active states, in which different agonists bind with high affinity and activate independent signaling pathways.[7] Moreover, it exists in inactive states followed by an internalization process in which it binds antagonists and inverse agonists (specifically ARBs) with high affinity.[8]

Table 1. ^{1}H NMR Chemical Shifts of Angiotensin II TFA Salt and Angiotensin II Acetate Salt (Human) in DMSO-d_6 at 600 MHz

						Angiotensin II TFA Salt				
	NH	αH	βH	β'H	γH	γ' H	γCH$_3$	δH	εNH	2H, 4H	Ar.H
Asp	8.13	4.09	2.77	2.60							
Arg	8.54	4.33	1.58	1.44	1.44			3.05	7.56		
Val	7.78	4.15	1.90				0.73				
Tyr	7.99	4.47	2.77	2.60							2,6H: 6.99 3,5H: 6.57
Ile	7.85	4.10	1.62		1.32	1.03	0.72	0.74			
His	8.29	4.74	3.02	2.88						8.92, 7.34	
Pro		4.35	1.99		1,76			3.61, 3.43			
Phe	8.26	4.38	2.99	2.90							7.24, 7.23

						Angiotensin II Acetate Salt (Human)				
	NH	αH	βH	β'H	γH	γ' H	γCH$_3$	δH	εNH	2H, 4H	Ar.H
Asp	7.85	4.07	3.08	3.00							
Arg	8.40	4.25	1.53	1.38	1.72			2.97	8.35		
Val	7.98	4.01	1.81				0.71 0.59				
Tyr	8.31	4.42	2.80	2.70							2,6H: 6.97 3,5H: 6,57
Ile	7.85	4.07	1.64		1.32	0,97	0,69	0.71			
His	8.06	4.61	2.87	2.74						7.45, 6.83	
Pro		4.25	1.81	1.73	1.47			3.13, 3.47			
Phe	7.78	4.18	3.04	2.89							7.16, 7.10

Table 2. Interatomic Distance Constraints (10% Toleration) of AngII Acetate and TFA Salt Obtained from ROE Connectivities and Used in MD Simulations

angiotensin II acetate salt (human)		angiotensin II TFA salt	
atom connectivities	constraint distances (Å)	atom connectivities	constraint distances (Å)
His6 NH - Tyr4 αH	2.66 (2.39−2.93)	His6 NH - Tyr4 NH	3.36 (3.02−3.69)
Tyr4 Ar.3,5H - Arg2 δH	2.95 (2.66−3.25)	His6 αH - Tyr4 αH	3.19 (2.87−3.51)
His6 2H - Phe8 βH	3.47 (3.12−3.82)	Pro7 δH − Ile5 βH	3.92 (3.52−4.31)

During the last 15 years, there has been a vast development of AT$_1$R antagonists. All of them share some common structural features and can be described as derivatives of the first sartan in the market, losartan. They are designed to mimic the C-terminal group of AngII, thus expected to act in a similar way. Their action is based on their ability to displace the vasoconstrictive peptide AngII from the AT$_1$ receptor.[9]

In an effort to comprehend their stereoelectronic features, several studies have been already published[10−19] to compare the conformational properties of AngII and its antagonists, in most cases marketed drugs for the treatment of hypertension. Furthermore, several structure activity relationship (QSAR) and molecular docking studies have focused on AT$_1$R antagonists in order to gain information for the design of novel analogues of higher potency and fewer side effects.

In the present study, the conformational properties of human AngII acetate salt which is the commercial form of the octapeptide has been studied in comparison with AngII-trifluoroacetic acid (TFA) salt in an amphiphilic (DMSO) solvent, in order to choose an environment resembling the aqueous-membrane one[20,21] and to investigate the impact of different acidity conditions (acetate[22] and TFA[23] salts) on AngII conformation. Our scope was to explore major similarities and differences between putative conformations of AngII in solution and in the active site of the AT$_1$ receptor. Moreover, our target was to investigate possible ligand receptor interactions and induced rearrangement of the receptor's domains related to AT$_1$ receptor activation. To this extent, NMR spectroscopy, *in silico* docking, and Molecular Dynamics simulations have been employed.

■ RESULTS AND DISCUSSION

Structure Assignment. The results of the ^{1}H resonance assignment of AngII acetate and TFA salt are listed in Table 1. The proton−proton ROE connectivities were identified from 2D ROESY spectra (Figure 1 (A, B)). In both forms, along the entire backbone of AngII strong sequential ROE connectivities dαN$_{(i,i+1)}$ are observed. These are indicative of a predominant population of random coil conformation in DMSO-d_6 solvent. It is worth mentioning that no secondary structure elements can be identified since such indicative medium or long-range contacts are absent. From the plethora of ROE cross-peaks, three pairs were selected as the most important for the conformational properties of both AngII forms (Table 2) and were applied as constraints at the MD simulations on AngII.

Conformational Analysis − MD Simulations in Solution. Two representative, energy minimized conformations of AngII acetate salt were derived after MD simulations in accordance with the ROE distances, sharing some common conformational characteristics. The C-terminal residues His6-Pro7-Phe8 form a backbone bend implied by the ROE correlation between the H2 of His6 and the βH of Phe8. Another common bend is observed for both conformers at the backbone of Tyr4-Ile5-His6 due to the spatial vicinity of Tyr4 αH and His6 NH. The major difference lies on the orientation of the Arg2 side chain. The first one (blue in Figure 2) is energetically favored (potential energy = 107.8 kJ mol^{-1}) possibly due to the side chain stabilization by an H-bond between the Arg2 guanidine group and the His6 heterocyclic ring, while the other one (brown in Figure 2) orients the side chain in an opposite direction (potential energy = 117.3 kJ mol^{-1}). This
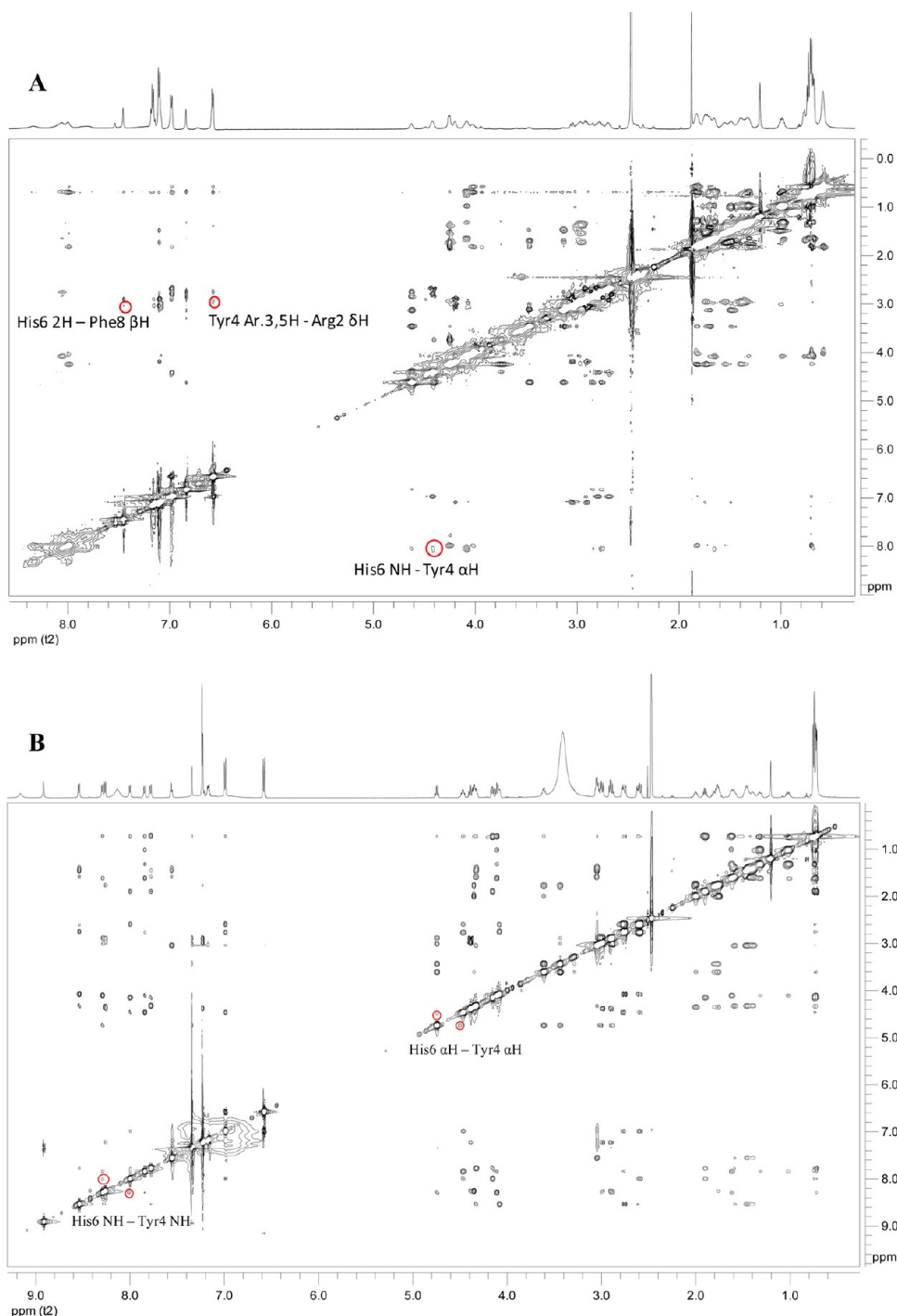
Figure 1. 2D ROESY spectra of (A) AngII acetate salt and (B) AngII TFA salt obtained in DMSO-d_6 at 25 °C. The calculated interproton distances from the crosspeaks marked in red circles were used as constraints for the MD simulations. (The cross-peaks for Pro7 δH − Ile5 βH are not observed at this contour-level display.)

flexibility of Arg2 induces a different conformation of the N-terminus of AngII (Figure 3). Despite this flexibility, the ROE distance calculated between the Arg2 δH and an aromatic proton of Tyr4 is satisfied in both cases.

In the case of the more acidic environment of TFA salt, the conformation of AngII is dominated by a large backbone bend (Tyr4-Ile5-His6-Pro7). The folded conformation of AngII derived from the MD simulations (Figure 4) is justified by the ROE signals between Tyr4 − His6 and Ile5 βH − Pro7 δH. This U-shaped structure resembles with the one found by Tzakos et

al.[24] in aqueous acidic solution (pH = 5.7), having though certain differences. In the case of the aqueous environment a hydrophobic cluster is formed by the Tyr4, Ile5, and His6 side chains on the one side of a plane defined by the peptide backbone, while in the case of the amphiphilic environment (DMSO) a cluster is created by Arg2, Tyr4, and Ile5 side chains and His6 is oriented away from the cluster (Figure 4).

Even though AngII acetate and TFA salt have major conformational differences in DMSO solution, both of them present a similar backbone bend at the C-terminal residues (His6
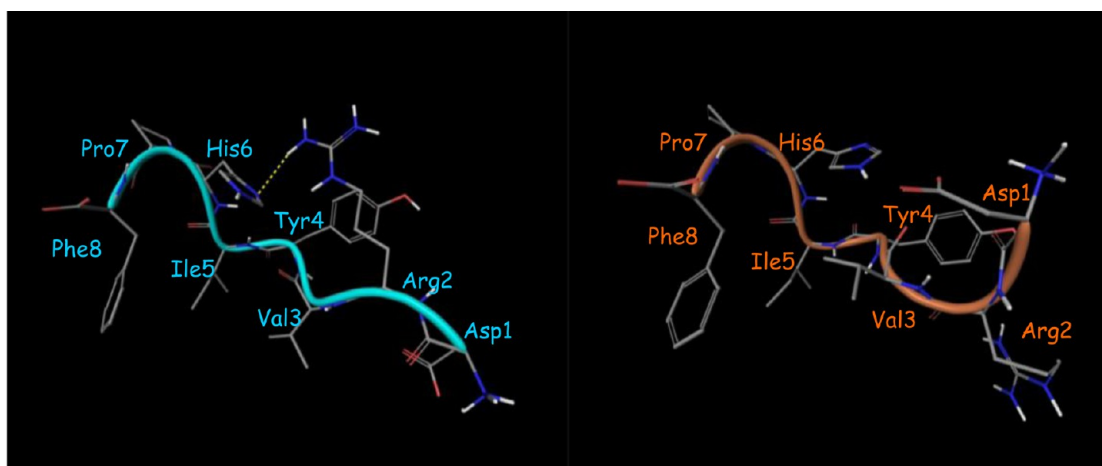
Figure 2. Two representative conformations of AngII acetate salt satisfying ROE distances after MD simulations.
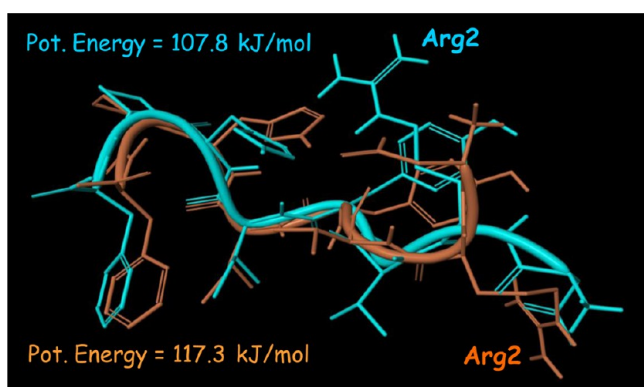

Figure 3. Superimposition of the two representative conformations of AngII from MD simulations depicting the flexibility of Arg2.
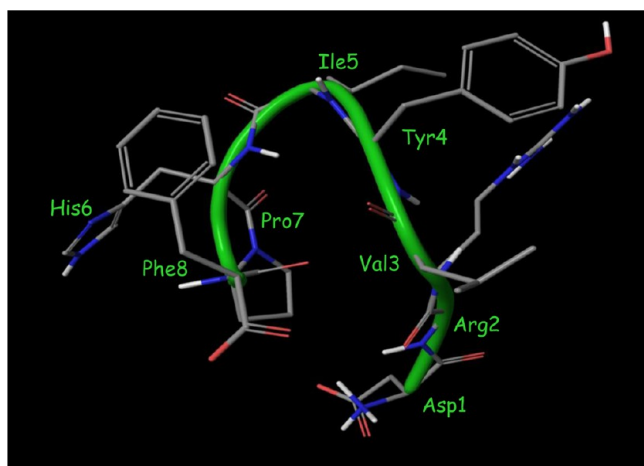

Figure 4. Representative conformation of AngII in accordance with the ROE distances of AngII TFA salt after MD simulations.

- Phe8). This finding is important since the C-terminus of AngII is crucial for AT_1 receptor binding and has been the template for the design of several inhibitors (sartans) during the last 2 decades.

The derived conformations of AngII acetate and TFA forms are available in pdb format.

Homology Modeling. There has been much discussion on the use of homology models of GPCRs,[25] and in many cases it has proven a valuable tool in virtual screening and drug design.[26] According to the phylogenetic analysis by Fredriksson and collaborators,[27] AT_1R belongs to the γ GPCR branch, which also includes the chemokine receptors among others. In particular, the CXCR4 crystal structure[28] represents the best possible crystal structure template available, sharing an overall amino acid percentage identity of 34% with the AT_1R, and, accordingly, it was used as a template. The conserved transmembrane GPCR residues were used as reference points for the sequence alignment (see the Experimental Section). The CXCR4 receptor retains most of the common GPCR structural characteristics, whereas the fourth transmembrane domain (TM4) differs in length as it forms an extra α-helix turn near the extracellular part. Due to the tertiary structure of the crucial ligand affinity second extracellular loop (ECL2), the extracellular tip of the TM4 domain is shifted toward the binding site (~3 Å) from its consensus position in other GPCRs. In this way, $R167^{4.64}$, a crucial residue for AngII binding,[29,30] is introduced to the binding site cavity. In the case of the chemokine receptor, the ECL2 β-strands are located near TMs 2 and 3 and are more exposed to the extracellular environment, interacting with the ligands in the binding site.[28] The crystal structures of the four opioid receptors (OPRL, OPRK, OPRD, and OPRM) and the neurotensin receptor (NTSR1) that also belong to the γ branch also suggest the β sheet formation in the ECL2 among all these subfamilies that possibly assists the accommodation of endogenous peptides. For the above reasons, ECL2 was left in the β sheet formation as in the template structure.

***In Silico* Docking on the AT_1 Receptor Site and MD Simulations.** Several studies have been performed focusing on the binding mode of angiotensin II receptor antagonists, in order to provide insights for the design of novel drugs. These studies have been using homology models of the receptor based on other GPCR resolved structures. Here we focus on the native octapeptide, performing *in silico* binding studies and MD simulations on the AT_1 receptor. A general overview of the molecular modeling techniques used in this study is presented in Figure S1.

Different starting complexes of the AngII-AT_1 receptor include (a) those with AngII from NMR and MD in solution, manually placed at the active site, and (b) those derived from flexible docking studies using an incremental approach (for the latter, see text Incremental construction of docking poses and
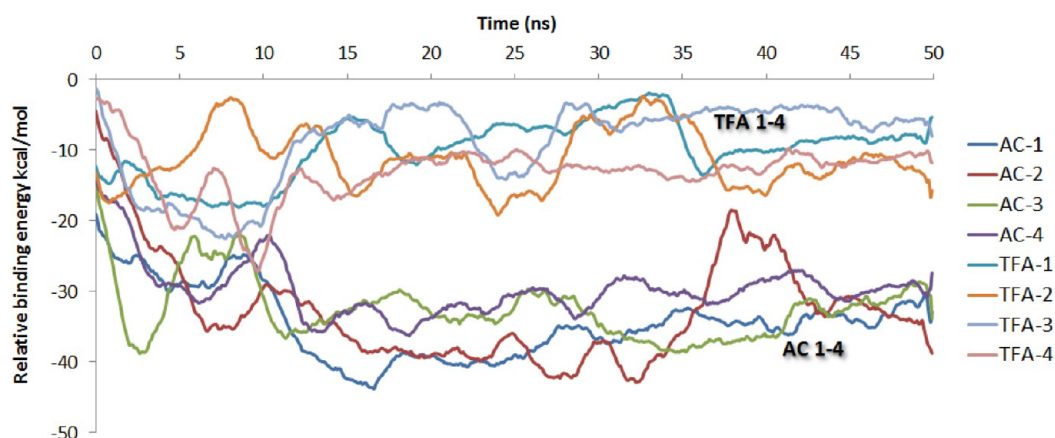
Figure 5. Relative binding free energies of differently docked conformations of angiotensin II to the AT1 receptor. The TFA NMR docked conformations show significantly less binding potential than the acetate conformation in all cases. Binding free energies are expressed in kcal mol^{-1}.
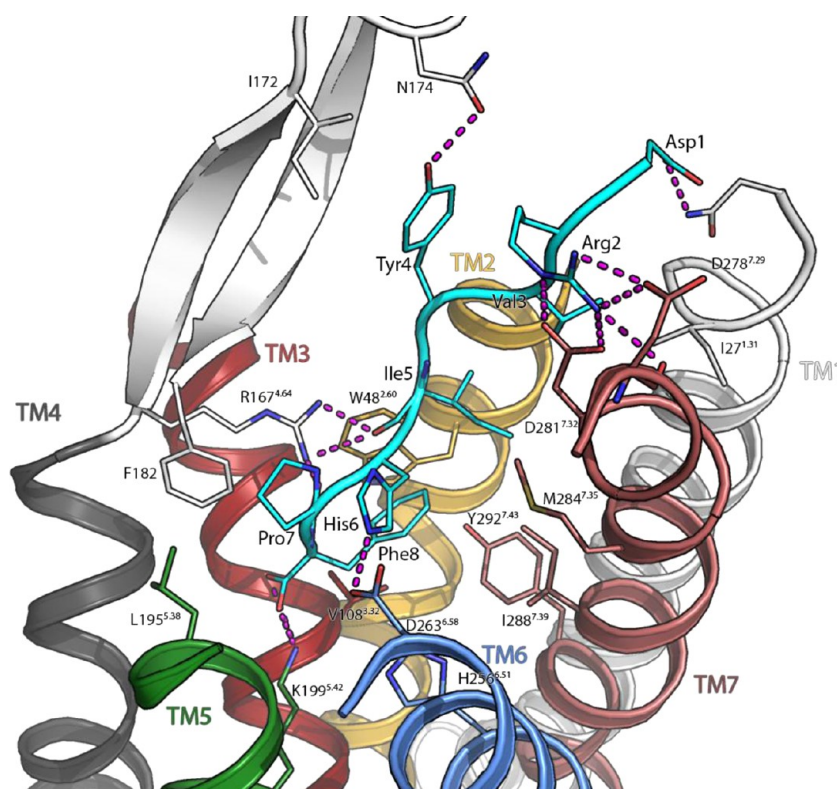

Figure 6. Representative conformation of the interaction between AngII (cyan) and AT1 after various MD simulations on the different acetate and TFA NMR structures (AC-1 complex). The depicted complex was extracted as the most favorable, having a stable MD profile and highest binding free energies. EL1, part of EL2 and EL3 are not shown for better clarity of the interaction. Helices color code: TM1 white, TM2 yellow, TM3 red, TM4 gray, TM5 green, TM6 blue, and TM7 brown.

MD simulations). All simulations were performed in the lipid bilayer environment (see the Experimental Section for details).

Two AngII conformations derived from NMR and MD (one for the acetate and one for the TFA salt) were manually placed into the active site in accordance to previous results from mutational and photolabeling studies on the AT$_1$ receptor.[31−33] More specifically, the carboxyl terminal group was oriented toward the polar side chain of K199$^{5.42}$ in TM5 (superscripts in protein residues correspond to the Ballesteros and Weinstein nomenclature[34]) as it has been found to be one of the most important contacts upon binding of several antagonists, including [Sar^1,Ile^8]AngII and especially AngII,[35] forming an ionic interaction. The recent crystal structure of part of the

natural peptide neurotensin bound to its receptor[5] was also used to provide important structural insights on endogenous peptide − GPCR interactions.

On this basis, four individual placements for each of the two NMR derived conformers were set as starting complexes, without making any spatial modifications to residues 3−8. In some cases, some minor changes were applied to the side chains of residues Asp1 and Arg2 to avoid steric clashes and accommodate the peptide in the receptor's binding site in the best possible way.

The binding free energies of AngII to the AT$_1$R, obtained by using the Linear Interaction Energy Method (LIE),[36] revealed more favorable interactions for the acetate conformation derived
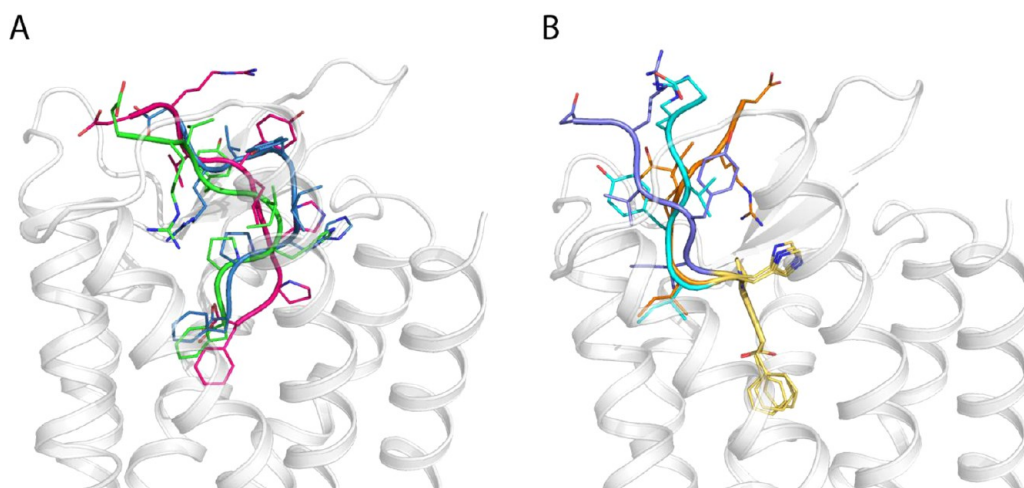
Figure 7. Best docked poses using the induced fit docking procedure. A) AngII docked conformations IFD-A (blue), IFD-B (red), and IFD-C (green). B) Lowest DOPE conformations of AngII after *ab initio* construction of the rest of the peptide on the induced fit docking of AngII(6-8) segment (yellow). The IFD(6-8)-A five N-terminal added residues are represented in dark blue, IFD(6-8)-B added residues in cyan, and IFD(6-8)-C added residues in orange. Colors correspond to those of Figure 5.
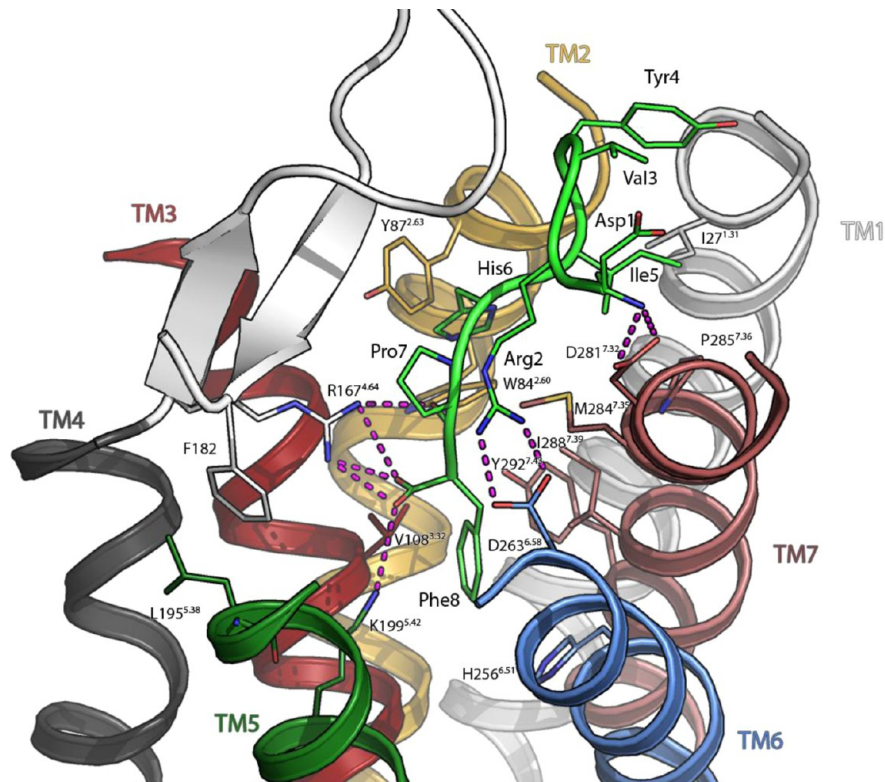

Figure 8. Representative low energy snapshot from the MD of the IFD-A complex, showing the interaction between AngII (green) and AT1. EL1, part of EL2 and EL3 are not shown for better clarity. Helices color code is as in Figure 6.

from NMR and MD studies (Figure 5). This can be explained through the more extended conformation of the acetate compared to the "U turn" conformation of the TFA salt. Moreover, the core of the binding site defined by the upper part of the transmembrane helices cannot accommodate the size of a folded conformation of the octapeptide. This can explain the notable differences in binding free energies after the first nanoseconds between the TFA and acetate conformations of $\sim$20 kcal mol^{-1}. In support of these results, all four trajectories of the bound TFA conformation, displayed very low stability in the organization of the 7TM helices of the AT$_1$ receptor (data not

shown). All the MD trajectories were visualized thoroughly whether they fulfilled known experimental data (mainly stability in the carboxyl terminal $-$ K199$^{5.42}$ interaction and a steady polar interaction with R167$^{4.64}$). The first complex (AC-1), which showed the best and most stable binding free energy values through the MD simulations, was chosen for further investigation.

As presented in Figure 6, the representative binding conformation of AngII shows an ionic interaction between K199$^{5.42}$ in TM5 and the carboxyl terminal of the peptide. The Phe8 bulky ring is oriented toward the highly hydrophobic
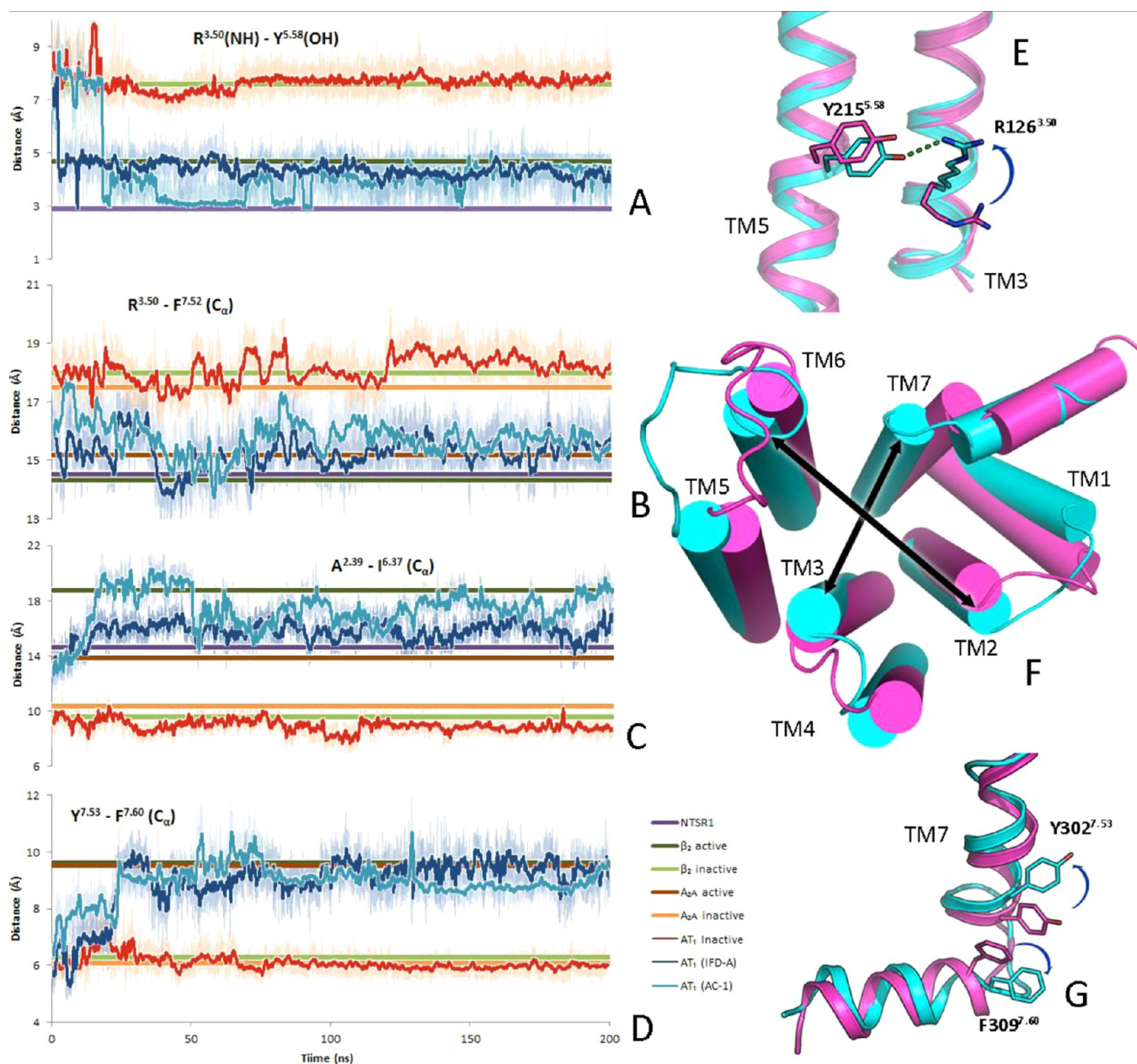
Figure 9. (A) Evolution of the $R^{3.50}$(NH) and $Y^{5.58}$(OH) functional groups distance, which interact upon activation in the β_2 adrenergic and neurotensin agonist bound states; (B) Evolution of the distance between $R126^{3.50}$ and $F301^{7.52}$ C_{α}'s, which depicts the small inward TM7 movement upon activation of the receptor; (C) Distance between TM2 and TM6 evolution, measured as the distance between the C_{α}'s of $A63^{2.39}$ and $I242^{6.37}$; (D) Evolution of the distance between $Y302^{7.53} - F309^{7.60}$ C_{α} atoms, in comparison with the β_2 adrenergic ($Y^{7.53} - F^{7.59}$), A_{2A} adenosine antagonist bound and β_2 adrenergic, A_{2A} adenosine and neurotensin agonist bound states; (E) Snapshots of the AC-1 complex showing the rotamer switch of $R126^{3.50}$ that occurs after ~18 ns of simulation time. The TM3 and TM5 helices of the AT1 receptor are shown in its inactive (magenta) and active (cyan) state; (F) Relative movements of the cytoplasmic part of the 7 TMs, as observed through the MD trajectory of the AC-1 complex. The starting conformation of AT1 is colored magenta and the final conformation in cyan. An inward movement of TM7 was observed, as well as the growing distance between TM2 and TM6; (G) Snapshots at 1 ns (magenta) and 70 ns (cyan) showing the increase in distance that occurs between $Y302^{7.53}$ and $F309^{7.60}$ during the MD simulations of the AT1 − AngII (IFD-A) complex.

pocket formed by residues $W84^{2.60}$ in TM2, $V108^{3.32}$ in TM3, $M284^{7.35}$, $I288^{7.39}$, and $Y292^{7.43}$ in TM7. Another important interaction is depicted between the carbonyl oxygens of Pro7 and Ile5 of AngII and $R167^{4.64}$ in TM4. This interaction is critical, since studies have shown an almost complete loss of AngII affinity when $R167^{4.64}$ was mutated.[29,30] In the present homology model, $R167^{4.64}$ points to the binding site core, adding a second positively charged residue to the cavity, interacting with the peptide's backbone. His6 interacts with the charged side chain of

$D263^{6.58}$ in TM6, while Pro7 interacts with F182 of the extracellular loop 2 (ECL2). $D263^{6.58}$ mutation has also been reported to almost abolish binding of the antagonistic peptide [Sar^1,Ile^8]AngII to the AT_1R.[37] The two hydrophobic residues Val3 and Ile5 of AngII appear to point toward the hydrophobic cleft mentioned above and form several van der Waals interactions. Tyr4 is found to interact with the ECL2, while Arg2 forms several polar interactions with the two negatively charged residues of TM7, $D278^{7.29}$, and $D281^{7.32}$ which have

been documented as important for full agonism of AngII.[32] The suggested orientation of Arg2 toward TM7, by forming polar interactions with D281[7.32], has been also reported recently by Fillion et al.[38]

Incremental Construction of AngII Docking Poses and MD Simulations. An incremental construction procedure was performed on AngII (see the Experimental Section) to produce AngII-AT$_1$R binding complexes. This iterative method begins with the docking of the truncated AngII C-terminal, comprised of three residues (AngII 6-8), followed by the addition of the rest amino acids one by one. After the stepwise addition of each residue, flexible docking is performed. From this procedure, three binding poses were selected (IFD-A,B,C) and are presented in Figure 7A.

Alternatively, the addition of the 5 remaining residues of AngII was performed in one step, on the binding pose of AngII 6-8, by applying the DOPE loop refinement module of the MODELLER v9.7 software (see the Experimental Section for details).[39] Specifically, the docked tripeptide (AngII 6-8), was held rigid, while the remaining five residues of the N-terminal domain were considered as a loop, for which, several models where computed.

The three lowest DOPE energy conformations (IFD(6-8)-A,B,C) (Figure 7B) along with the three best poses from the incremental construction using IFD (IFD-A,B,C) (Figure 7A) were further subjected to MD simulations in the lipid bilayer environment, as was previously done for the NMR conformations (Figure S1). Comparing the relative binding free energies during the MD simulations, the IFD-A conformation showed the best overall interaction energy (Figure S2), even better than the AC-1 conformation, suggesting a more probable binding mode for AngII.

Figure 8 depicts the representative interactions that appeared during the optimal binding energy values of the IFD-A MD simulation. Phe8 has a similar interaction pattern, interacting with the core hydrophobic residues V108[3.32] and I288[7.39] as well as H256[6.51]. K199[5.42] forms strong polar interactions with the carboxyl terminal group, which also interacts with R167[4.64]. The latter also forms a hydrogen bond with the backbone of Pro7. Again, there is a hydrophobic set of interactions between Ile5 and the residues of the TM1 and TM7 hydrophobic cleft I27[1.31] and P285[7.36], for which has been shown that when mutated, no detectable binding to [Sar[1],Ile[8]]AngII is observed.[40] In comparison to the acetate docked conformation, no specific interactions are observed for Val3, while the N-terminus interacts with the side chain of D281[7.46]. Arg2 reaches for D263[6.58], to form a salt bridge as it has recently proposed elsewhere,[38] while in the acetate conformation it contacts the two aspartic acids of TM7. This could serve as a hypothesis for the role of Arg2, stabilizing the active state of the receptor by anchoring to the side chains of the three aspartic acids on TM6 or TM7 that are crucial for AngII agonism.

A recent study by Fillion et al.[38] suggests a somewhat vertical binding mode of AngII at AT$_1$R, similar to our results, with the N-terminal interacting across the extracellular surface and the C-terminal interacting more deeply within the transmembrane domain core. This similarity is supported by the presence of the hydrogen bond between Phe8 - K199[5.42] and the salt bridge Arg2 - D263[6.58] for both cases. Furthermore, both studies suggest the importance of the Arg2 interactions with the negatively charged residues of TM6 and TM7 that are known to bind AngII and its derivatives.[32,37]

On the other hand, Fillion et al. propose a close contact of Phe8 to W253[6.48] instead of R167[4.64], which participates in a

hydrogen bonding network with Tyr4 and His6. Val3 is located right in front of His183[i+3] and is surrounded by the hydrophobic residues Ile172[i-8], Val179[i-1], Ala181[i+1], and Tyr184[i+4], which is not the case in our study (positions i+1, i+2, etc., refer to residues of the ECL2 relative to the conserved C180[i], forming a disulfide bond with C101[3.25] in TM3). Interestingly D281[7.32] forms a hydrogen bond with Arg2, while in our study this bond is formed with Asp1, indicative for the approach of the AngII N-terminal to TM7.

MD Simulations and Receptor Activation. It is widely accepted that the activation of GPCR's is a dynamic process. The energy landscape of the β_2 adrenergic receptor has been extensively studied through the use of ABEL trapping[41] and NMR spectroscopy combined with MD simulations,[42] showing that GPCRs exist in different inactive and active states, depending on the presence of an agonist, antagonist, insurmountable antagonist, or a G protein. The crystallographic structures of antagonist and agonist bound β_2 adrenergic receptor[3,43] display minor changes in the binding site but notable movements in the intracellular part of the helices. Apart from the ionic interaction, in which, upon activation R[3.50] switches the position of its side chain to interact with Y[5.58], a 14 Å outward movement is observed at the cytoplasmic end of TM6. Moreover, an inward movement of the cytoplasmic part of TM7 is observed toward the binding of the G protein, and a small increase in the distance between TM3 and TM5 is measured from the distance of the C$_\alpha$ atoms of R[3.50] and I[5.61]. In the agonist bound states of A$_{2A}$ adenosine,[4] β_2 adrenergic,[3] and neurotensin[5] receptors, in the absence of a G protein, these changes are visible but not to the same extent. This can be explained by the synergistic way an agonist and the G protein act in order to induce these structural reorientations of a GPCR's cytoplasmic counterparts.

To study these agonist induced mechanistic reorientations for the case of the membrane embedded AT$_1$ receptor, we monitored the aforementioned changes extending the MD simulations of AC-1 and IFD-A complexes to 200 ns. An MD simulation of the receptor in its inactive state was performed for comparison reasons, as well as a simulation on the crystal structure of CXCR4 with its antagonist IT1t as a positive control for the homology model rmsd values of these MDs are reported in Figure S3. Several spatial elements were monitored during simulations (Figure 9), which summarize the dynamic changes, which were observed in the conformational behavior of the protein, induced by the presence of the endogenous agonist AngII.

The R126[3.50] − D125[3.49] intrahelical salt bridge, which exists in the inactive state of most GPCR crystal structures, is broken upon activation, allowing R[3.50] to form an interhelical hydrogen bond with the conserved Y215[5.58]. This R126[3.50] − D125[3.49] interaction breaks in both simulations in different time intervals, in which Y215[5.58] orients its side chain toward TM3 to form a stable hydrogen bond interaction with R126[3.50] (Figure 9 (A, E)). Another dynamic event that takes place upon activation in crystallized GPCRs is a slight inward movement of the cytoplasmic part of TM7. Throughout our simulations, this movement was measured as the distance between C$_\alpha$'s of R126[3.50] and F301[7.52] which is gradually decreased in both AC-1 and IFD-A complexes' simulations to a final of ∼15 Å as in the crystal structure of the $\beta_2$andrenergic, A$_{2A}$ adenosine, and neurotensin type 1 (NTSR1) receptor's active state. In the agonist bound crystal structures, the largest observed movement is the outward TM6 cytoplasmic movement. In the present MD
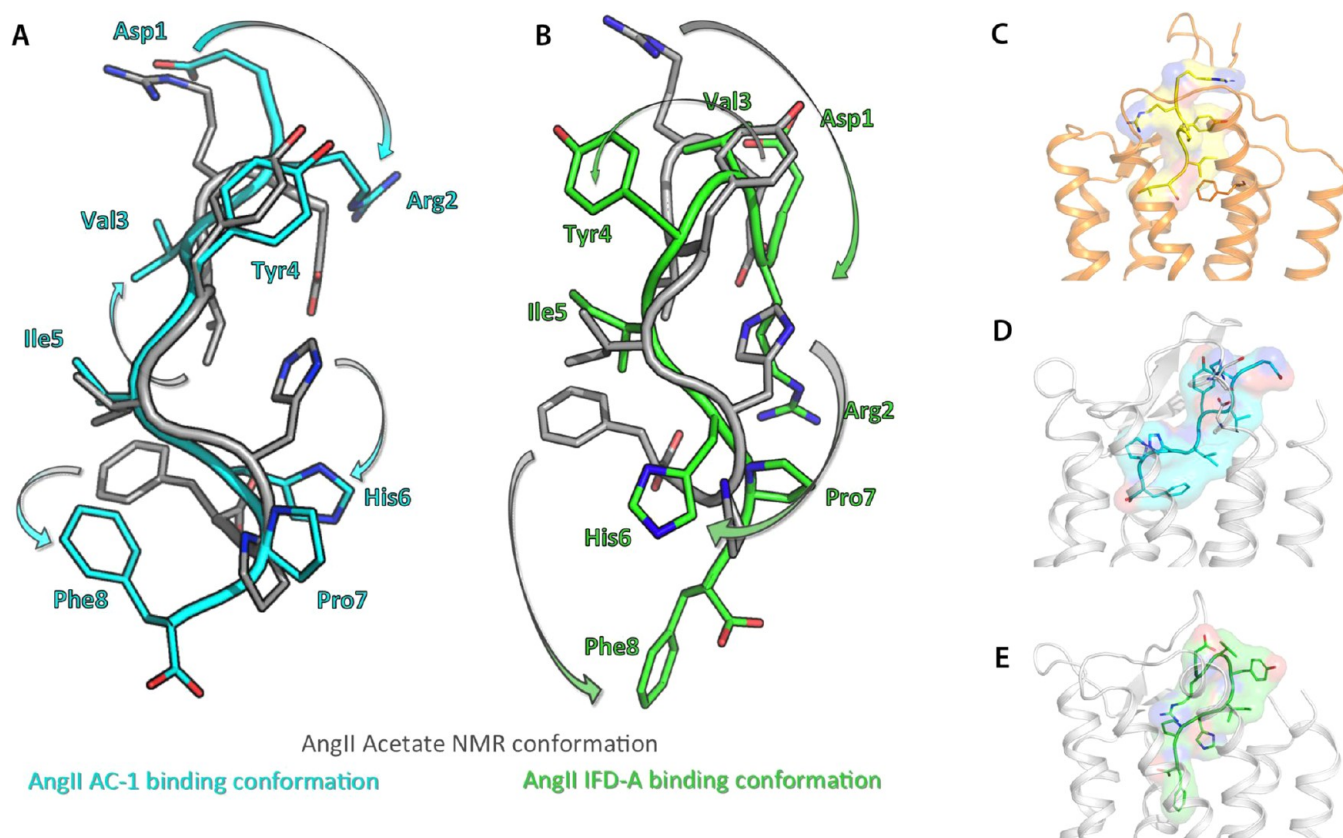
Figure 10. (A) Conformational transitions of the (NMR derived) AngII (acetate salt) in solution (gray) to its bound conformation in the AT1 receptor (cyan); (B) Conformational differences between the solution structure of AngII (gray) and the binding representative conformation of docked (IFD-A complex) AngII (green) after MD simulations; (C) Binding orientation of neurotensin bound to the NTS1 receptor in orange ribbon style (pdb code 4GRV); (D) The AC-1 complex orientation of AngII presented in cyan; (E) The IFD-A AngII orientation in green.

simulations, this movement was measured as the distance between $A63^{2.39}$ and $I242^{6.37}$ and was found to be constantly increasing for the first 20 ns. Even though in the starting conformations of these models TM6 was manually tilted outward (see the Experimental Section), an extended movement was observed, along with a small movement of the TM2 intracellular part (Figure 9 (C, F)). Another dynamic element observed in GPCRs' activation is the increase of the $Y^{7.53} - Y^{7.60}$ distance, resulting in the TM7−H8 conformational rearrangement.[44] This distance was observed to increase gradually in both simulations (AC-1 and IFD-A), starting from ∼6 Å, to reach a value of ∼9 Å after the first 20 ns and remained stable for the rest of the trajectory (Figure 9D). Recently, the potential formation of a specific H-bond has been proposed between residues $D74^{2.50}$ and $N46^{1.50}$ during activation of the AT_1 receptor,[45] which are located deeper in the transmembrane domain. However, this hydrogen bond was not observed through the MD simulations as $D74^{2.50}$ is constantly interacting with $N111^{3.35}$.

Comparing these conformational changes to the *apo* form of AT_1R (inactive state) during simulation, it is obvious that the presence of AngII is responsible for dynamic changes in the topology of the receptor. Most of these changes occur in the intracellular part and resemble the changes observed during the activation of other GPCRs. Although two different binding orientations of AngII were found, the conformational spaces visited by these peptide bound complexes were similar and considerably distinct from those of the inactive state MD simulation.

Angiotensin II Conformational Elements. The two preponderant bound conformations of AngII (NMR derived and IFD-A) also undergo a series of conformational changes during the MD simulations. In both 200 ns simulations, the backbone root-mean-square deviation (rmsd) of the receptor is stable between 0.3 and 0.4 nm, whereas the NMR conformation of AngII is stabilized at a backbone rmsd value of ∼0.18 nm (Figure S3). This can be explained through the fact that the acetate conformation was manually docked without changes in its initial, based on NMR, topology. Therefore, during the first ∼20 ns of the simulation, it is rearranging to its putative active conformation in the receptor's binding site. The induced fit docking conformation of the peptide (IFD-A), however, demonstrates lower backbone rmsd values of ∼0.10 nm during the first 24 ns, which increase at a later point to ∼0.14 nm to remain steady for the remainder of the simulation. The inactive state of the receptor is more stable, having a constant rmsd backbone value of 0.2 nm after the first 80 ns.

In order to evaluate the conformational changes of AngII upon binding to the receptor, we used the NMR structure of AngII acetate salt in DMSO, since it may resemble the conformation of the unbound AngII (in an amphiphilic environment).

This starting solution of the NMR acetate structure was compared with the two predominant bound conformations (Figure 10). Calculating the rmsd between the NMR structure and the optimal binding conformation of AngII after the corresponding MD simulation (AC-1), there is no major change in the topology of the backbone atoms of the peptide (rmsd = 0.21 nm). However, the overall backbone atoms rmsd has a value

2806

dx.doi.org/10.1021/ci4003014 | *J. Chem. Inf. Model.* 2013, 53, 2798−2811

of 0.46 nm and is mostly affected by the movement of the terminal residues Asp1, Arg2, and Phe8, which accommodate their functional groups in the binding cavity during the first nanoseconds of the simulation. Naturally, the best unconstrained conformation of AngII, IFD-A, has a more different topology than the NMR acetate structure, with backbone and non-hydrogen rmsd of 0.31 and 0.57 nm respectively. This conformation exhibited slightly better binding free energies than AC-1 and similar binding characteristics for the last three residues His6-Pro7-Phe8.

MD simulations demonstrate that AC-1 undergoes several conformational alterations upon binding (Figure 10A). These include the positional switch of Asp1 and Arg2 side chains in order to interact with the binding site. Asp1 is oriented toward TM1 and Arg2 toward the two aspartic acids $D278^{7.29}$ and $D281^{7.32}$. Another change refers to the orientation of the Phe8 carboxyl group, which forms an ionic interaction with $K199^{5.42}$. Furthermore, the His6 side chain flips so that its imidazole group interacts with TM6. The IFD-A final conformation presents greater changes than AC-1 with respect to the solution conformation, mainly including changes of the aforementioned terminal residues Asp1, Arg2, His6, and Phe8 (Figure 10B). Furthermore, small alterations are also observed in Val3 and the side chain of Tyr4. However, in both binding conformations of AngII, the backbone in positions Tyr4-Ile5-His6-Pro7 does not change to a great extent regarding the solute conformation.

To date, there are two crystal structures of peptides interacting with GPCRs. The CXCR4 receptor bound to CVX15 peptide antagonist[28] and the NTSR1 receptor bound to its endogenous peptide agonist neurotensin,[5] being the first reported binding mode of a peptide agonist to a GPCR. Neurotensin binds to its receptor (Figure 10C), in a mode similar to the two AT$_1$R-AngII binding propositions (Figure 10 (D, E)). This observation could support the existence of a common interaction pattern in peptide − GPCR complexes.

First, the terminal residue Leu13 of neurotensin is accommodated in the area between TM3, TM5, TM6, and TM7, with the carboxyl group forming an ionic interaction with $R^{6.54}$ and the hydrophobic side chain resting between $F^{6.58}$ and $I^{5.42}$. In our putative interactions, the carboxyl terminal group interacts with $K199^{5.42}$, in a similar position, while the Phe8 aromatic ring interacts with $I288^{7.39}$, $V108^{3.32}$, and $H256^{6.51}$.

Ile12 of neurotensin interacts with TM2 and TM7 hydrophobic residues (mostly $F^{2.65}$ and $Y^{7.35}$), and Tyr10 features its side chain oriented toward the ECL2. In our models, Ile5 and Tyr4 of AngII have similar profiles, Ile5 interacts with several TM1, TM2, and TM7 residues, while Tyr4 occupies the same position in the AC1 complex. The two arginine residues of neurotensin, Arg8 and Arg9, contact several TM6 and TM7 ectodomains, while in both cases of the present study Arg2 is depicted anchoring to the extracellular TM6 and TM7 aspartic acids $D263^{6.58}$, $D278^{7.29}$, and $D281^{7.32}$.

■ CONCLUSIONS

This study investigates the AngII binding mode at the AT$_1$ receptor and gains insights into its activation mechanism. Crucial interactions of AngII upon binding were investigated employing several MD simulations with AngII conformations derived from NMR data and *in silico* docking studies. A homology model of the AT$_1$ receptor based on the crystal structure of the CXCR4 chemokine receptor was used since no crystallographic structure is still available.

Of major importance, was to investigate whether the already known structural rearrangements of GCPRs are reproduced during MD simulation for the AT$_1$ receptor upon activation induced by its natural agonist.

Comparing the conformational changes of the active to the inactive AT$_1$R, it can be deduced that the presence of AngII is responsible for dynamic changes in the topology of the receptor. Most of these changes occur in the intracellular part of the receptor and resemble the changes observed in GPCR activation. Indicatively, the intrahelical salt bridge between $R126^{3.50}$ and $D125^{3.49}$ in TM3, which exists in the inactive state of GPCRs, is broken upon activation, allowing $R126^{3.50}$ to form an interhelical hydrogen bond with the conserved residue $Y215^{5.58}$ in TM5. Another dynamic event observed for AT$_1$R, which takes place upon activation in crystallized GPCRs, is a slight inward movement of the cytoplasmic part of TM7.

The putative bioactive AngII conformer IFD-A with the best relative binding free energy during the MD simulations has certain common interactions with AT$_1$R as in the recently published model by Fillion et al..[38] Our results demonstrate the role of $K199^{5.42}$ of the fifth transmembrane helix (TM5), one of the most important residues for binding, forming strong polar interactions with the carboxyl terminal of AngII. The phenyl group of Phe8 interacts with the core hydrophobic residues $V108^{3.32}$ of the TM3 and $I288^{7.39}$ of the TM7, while Arg2 reaches to the side chain of the aspartic acid on TM6, which is crucial for AngII agonism. Moreover, the very important residue, $Arg167^{4.64}$, forms strong polar interactions with the C-terminal and the backbone of the peptide.

Another important aspect of the present study is the use of CXCR4 as a template for modeling accurate models of AT$_1$R, where the $Arg167^{4.64}$ is introduced in the binding site. This occurrence is due to the extra helical turn in the extracellular part of TM4 presented in the recent crystal structures of peptide-activated GPCRs. The introduction of $Arg167^{4.64}$ in the active site has been proven crucial for the stabilization of the peptide ligand.

Interestingly, many similarities were observed between our model and the binding mode of neurotensin to the NTSR1 in the recently published crystal structure. First, the hydrophobic C-terminal residues of both peptides are accommodated between TM3, TM5, TM6, and TM7, forming a polar interaction with a positive charged residue, $K199^{5.42}$ for AT$_1$R and $R167^{4.64}$ for NTSR1. Second, several anchoring polar contacts were observed between the peptide and the receptor's TM6 and TM7 ectodomains, mainly Arg2 of AngII to the aspartic acids $D263^{6.58}$, $D278^{7.29}$, and $D281^{7.32}$ of the AT$_1$R resembling the Arg9 contacts of neurotensin to $F^{6.58}$ and $D^{6.63}$ of NTSR1.

The observed conformational reorientations from AngII in solution to its putative binding conformations could be of importance regarding the conformational characteristics of the peptide. The bend caused by Pro7 appears to be maintained upon binding to a lesser extent and the turn around residues Tyr4-Ile5-His6 was unchanged in both binding proposals during the MD simulations. These observations, based on NMR experiments and extended MD simulations, indicate that AngII undergoes minor changes in the backbone residues 3−6 and major changes in the terminal residues Asp1, Arg2, and Phe8 upon binding to the AT$_1$ receptor.

■ EXPERIMENTAL SECTION

NMR Spectroscopy. Angiotensin II (human) acetate salt was purchased by Sigma-Aldrich, Inc. (St. Louis, USA), while

angiotensin II TFA salt was synthesized by Prof. Matsoukas' group, Chemistry Department at University of Patras (Greece). NMR spectra were recorded on a Varian 600 MHz spectrometer. The sample concentration used in NMR studies was ca. 6 mM dissolved in DMSO-d_6. Two dimensional homonuclear (TOCSY, ROESY) NMR techniques performed with gradients were used to structurally elucidate the two forms of AngII. 2D ROESY experiments were carried out using a mixing time of 75 ms, which ensures the operation at the initial linear part of the NOE buildup curve and the PRESAT sequence in order to suppress the water signal. 2D TOCSY experiments were performed using a spin-lock time of 80 ms. The spectral width (SW) used was 6600 Hz. The 2D spectra were obtained with 64−128 scans in t2 dimension, 256 increments in t1 dimension, and a relaxation delay of 1 s.

Experimental data were processed using MestReNova 6.0.1 software. Interatomic proton−proton distances were calculated using the two-spin approximation, and the integrated cross-peak intensity of the germinal pair of protons ($\delta-\delta'$) of Pro7 was assumed to have a distance of 1.78 Å. The resulting distances were corrected for the frequency offset effects to be eliminated.[46] Upper and lower limit values of constraints were allowed (10% of toleration).

Conformational Analysis. Computer calculations were performed in a High Performance Computing (HPC) 64bit Grid (24 cores) based on Sun Grid Engine's Parallel Computing software, using Schrodinger Suite 2012 molecular modeling package. More specifically, Molecular Mechanics calculations were performed under Macromodel,[47] using the OPLS 2005 force field. AngII was first minimized with the PRCG (Polak-Ribiere Conjugate Gradient) algorithm using 2000 iterations and an energy tolerance of 0.01 kcal mol^{-1} Å^{-1}, to reach a local minimum. The dielectric constant (ε) was set to 47 during minimization, simulating the DMSO environment of the NMR solvent. The conformational space of AngII was explored using Molecular Dynamics. An implicit solvent model was applied, along with the SHAKE algorithm, which was also implemented to satisfy bond geometry constraints and keep fixed bond lengths during all simulations. The simulation temperature was 300 K with time step of 1 fs, equilibration time of 2 ns, and simulation time of 15 ns. 1000 conformers were extracted and clustered in 10 groups based on their phi, psi, and omega dihedral angles. The ones that satisfied as many as possible crucial ROE interatomic distances were selected and subjected again in Molecular Dynamics under the same parameters, where all the critical constraints of Table 2 were applied. The lowest energy conformers of the 10 derived clusters were thoroughly examined in order to select those with the best fit to the restrained distances.

Homology Modeling - Refinement. The primary sequence of the AT$_1$ receptor was obtained from the Universal Protein Resource (UNIPROT) database[48] (UNIPROT ID: P30556). The CXCR4 crystal structure[28] (PDB ID: 3ODU; 2.50 Å resolution) was used as a template for the homology model of AT$_1$R. Alignment was performed manually taking into account the highly conserved amino acid residues N$^{1.50}$, the LAxAD (L$^{2.46}$, A$^{2.47}$, A$^{2.49}$, and D$^{2.50}$) and DRY (D$^{3.49}$, R$^{3.50}$, and Y$^{3.51}$) motifs, the tryptophan in the fourth helix W$^{4.50}$, the two prolines P$^{5.50}$ and P$^{6.50}$, and the NPxxY motif in TM7 (N$^{7.49}$, P$^{7.50}$, and Y$^{7.53}$). These regions were used as reference points for the sequence alignment. The homology model was built using MODELLER v9.7,[39] and the construction of the receptor involved the disulfide bond between C101 and C180 in the extracellular domain, connecting

ECL2 and TM3. The intracellular part of TM5 was manually tilted outward in a topology resembling the active state of the β_2 adrenergic receptor[3] (PDB ID: 3SN6) in order to evaluate the changes induced in the receptor by the AngII peptide during the MD simulations. Moreover, because the CXCR4 crystal structure lacks a helical part in the H8 sequence of GPCR's, this final part of the model was built using the topology of the rhodopsin crystal structure[49] (PDB ID: 1GZM). The overall stereochemical quality of the final model was evaluated by thorough visual inspection, the discrete optimized energy (DOPE),[50] and the program PROCHECK.[51]

In Silico Docking. *In silico* docking studies were performed using Glide and Induced Fit Docking protocols.[52] The center of the initial grid was defined as the centroid of the following residues: V108$^{3.32}$, L112$^{3.36}$, Y113$^{3.37}$, R167$^{4.64}$, V179^{i-1}, F182^{i+2}, Y184^{i+4}, K199$^{5.42}$, N200$^{5.43}$, W253$^{6.48}$, H256$^{6.51}$, and Q257$^{6.52}$, which have been found to be important for the binding of AngII and/or AT$_1$ receptor antagonists.[31,33,53−56]

Since the carboxyl terminal part (residues 6-8) of AngII, is responsible for triggering biological activity (AT$_1$R antagonists were designed to mimic the C-terminal segment of AngII[9]), this segment was used to initiate the incremental construction procedure of the peptide in the active site. Thus, the first step of our incremental docking methodology was to perform Glide SP docking of the tripeptide (AngII 6-8). Top docking score binding poses of AngII 6-8, stabilized by the crucial interaction with K199$^{5.42}$, were used as a template for the addition of the next residue (I5). The new fragment (AngII 5-8) was docked using the Induced Fit Docking (IFD) protocol. IFD was comprised of three stages: i) the initial docking (Glide SP) using as center of the grid the AngII 6-8 best binding poses, ii) the refinement of the residues position within 5 Å from the ligand, utilizing Prime module, and iii) Glide SP redocking at the refined receptor. This iterative procedure was performed for all the remaining residues of AngII and was implemented in order to let the AT$_1$ receptor adopt better the induced conformational changes by the AngII binding.

The procedure of adding the remaining five residue segment (Asp1-Arg2-Val3-Tyr4-Ile5) of AngII after the induced fit docking of the tripeptide (His6-Pro7-Phe8) was performed using the DOPE-based *ab initio* loop modeling protocol.[57] The quality of the 1000 different peptide conformations in the presence of the receptor was evaluated with the DOPE (Discrete Optimized Protein Energy) method to conclude to the three lowest energy conformations.[50]

Molecular Dynamics. All MD simulations were performed using the GROMACS software v4.5.5.[58] Following the homology model, a minimization of the receptor topology was performed in order to remove steric clashes between the residues. The minimized topology was then inserted in a pre-equilibrated box containing a POPC lipid bilayer, water, and a 0.15 M concentration of Na$^+$ and Cl$^-$ ions with its long axis perpendicular to the membrane interface.[59] The latest AMBER99SB-ILDN[60] force field was used for all the dynamics simulations along with the TIP3P water model. In all simulations containing the membrane atoms, the lipid parameters described by Berger and co-workers were used[61] in a procedure recently validated.[62] Each system consisted of the protein, the peptide, 190 POPC molecules, ∼13.000 water molecules, and ∼130 ions in a 9 × 9 × 10 nm simulation box. The 14 model systems in total were energy minimized and subsequently subjected to a 1 ns MD equilibration, with positional restraints on protein coordinates. These restraints were released, and 50 ns MD trajectories were

produced in constant temperature of 300 K using separate v-rescale thermostats for the protein, the peptide, lipids, and solvent molecules. MD simulations for AC-1 and IFD-A complexes were extended to 200 ns. A total of 1 ms simulation time was performed for all trajectories. A time step of 2 fs was used, and all bonds were constrained using the LINCS algorithm.[63] Lennard-Jones interactions were computed using a cutoff of 10 Å, and the electrostatic interactions were treated using PME[64] with the same real-space cutoff. The linear interaction energy (LIE) method[36] was applied to monitor the interaction potential energy between the peptide and the receptor during the simulations. The LIE method has not been extensively applied to protein—protein interactions, but considering the equality of the systems studied (same ligand for the same target) and the small MW of AngII, it was used for comparison purposes of the different orientations of the same ligand. The optimized values for protein—protein interactions of 0.5 and 0.5 were used for the coefficients α and β respectively.[65]

■ ASSOCIATED CONTENT

Ⓢ Supporting Information

Figure S1: Summary of computational methods uses through the study. Figure S2: Relative binding free energies of angiotensin II docked by the IFD procedure to the AT1 receptor through the MD simulations. Figure S3: Root mean square deviations of AT_1 receptor and AngII backbone atoms, throughout the MD simulations. This material is available free of charge via the Internet at http://pubs.acs.org.

Ⓦ Web-Enhanced Feature

The derived conformations of AngII acetate and TFA forms are available in pdb format.

■ AUTHOR INFORMATION

Corresponding Authors

*E-mail: E-mail: pzoump@eie.gr (P.Z.) Corresponding author address: Institute of Biology, Medicinal Chemistry and Biotechnology, National Hellenic Research Foundation, 48 Vas. Constantinou Ave., 11635, Athens, Greece. Tel: +30210 7273 854

*E-mail: imats@upatras.gr (J.M.) Corresponding author address: Department of Chemistry, University of Patras, 26500 Patras, Greece.

Author Contributions

The manuscript was written through contributions of all authors. All authors have given approval to the final version of the manuscript. M.-T.M. and C.P. contributed equally.

Notes

The authors declare no competing financial interest.

■ ACKNOWLEDGMENTS

■ ABBREVIATIONS

RAAS, Renin Angiotensin Aldosterone System; AngII, angiotensin II; AT_1R, angiotensin II receptor type 1; GPCR, G-protein coupled receptor; ARB, angiotensin receptor blocker; TM, transmembrane domain; ECL2, extracellular loop 2; MD, molecular dynamics; NMR, nuclear magnetic resonance; ROE, rotating frame Overhauser effect; ROESY, rotating frame Overhauser effect spectroscopy; TOCSY, total correlation spectroscopy; TFA, trifluoroacetic acid; DMSO, dimethyl sulfoxide; CXCR4, chemokine receptor type 4; IP3, inositol trisphosphate; DAG, diacylglycerol; QSAR, quantitative structure—activity relationship; OPRL, nociceptin/orphanin FQ peptide receptor; OPRK, κ opioid receptor; OPRD, δ opioid receptor; OPRM, μ opioid receptor; NTSR1, neurotensin receptor type 1; LIE, linear interaction energy method; IFD, induced fit docking; rmsd, root mean squared deviation; HPC, high performance computing; OPLS, optimized potentials for liquid simulations; PRCG, Polak-Ribiere conjugate gradient; DOPE, discrete optimized energy; POPC, 1-palmitoyl-2-oleoylphosphatidylcholine; PME, particle mesh Ewald

■ REFERENCES

(1) Messerli, F.; Weber, M. A.; Brunner, H. R. Angiotensin II receptor inhibition: A new therapeutic principle. *arch. Intern. Med.* **1996**, *156*, 1957—1965.

(2) Goodfriend, T. L.; Elliott, M. E.; Catt, K. J. angiotensin receptors and their antagonists. *N. Engl. J. Med.* **1996**, *334*, 1649—1655.

(3) Rasmussen, S. G. F.; DeVree, B. T.; Zou, Y.; Kruse, A. C.; Chung, K. Y.; Kobilka, T. S.; Thian, F. S.; Chae, P. S.; Pardon, E.; Calinski, D.; Mathiesen, J. M.; Shah, S. T. A.; Lyons, J. A.; Caffrey, M.; Gellman, S. H.; Steyaert, J.; Skiniotis, G.; Weis, W. I.; Sunahara, R. K.; Kobilka, B. K. Crystal structure of the β_2 adrenergic receptor—Gs protein complex. *Nature* **2011**, *477*, 549—555.

(4) Xu, F.; Wu, H.; Katritch, V.; Han, G. W.; Jacobson, K. A.; Gao, Z.-G.; Cherezov, V.; Stevens, R. C. Structure of an agonist-bound human A_{2A} adenosine receptor. *Science* **2011**, *332*, 322—327.

(5) White, J. F.; Noinaj, N.; Shibata, Y.; Love, J.; Kloss, B.; Xu, F.; Gvozdenovic-Jeremic, J.; Shah, P.; Shiloach, J.; Tate, C. G.; Grisshammer, R. Structure of the agonist-bound neurotensin receptor. *Nature* **2012**, *490*, 508—513.

(6) Hunyady, L.; Catt, K. J. Pleiotropic AT1 receptor signaling pathways mediating physiological and pathogenic actions of angiotensin II. *Mol. Endocrinol.* **2006**, *20*, 953—970.

(7) Saulière, A.; Bellot, M.; Paris, H.; Denis, C.; Finana, F.; Hansen, J. T.; Altié, M.-F.; Seguelas, M.-H.; Pathak, A.; Hansen, J. L.; Sénard, J.-M.; Galés, C. Deciphering biased-agonism complexity reveals a new active AT_1 receptor entity. *Nat. Chem. Biol.* **2012**, *8*, 622—630.

(8) Gether, U. Uncovering molecular mechanisms involved in activation of G protein-coupled receptors. *Endocr. Rev.* **2000**, *21*, 90—113.

(9) Mavromoustakos, T.; Kolocouris, A.; Zervou, M.; Roumelioti, P.; Matsoukas, J.; Weisemann, R. An effort to understand the molecular basis of hypertension through the study of conformational analysis of losartan and sarmesin using a combination of nuclear magnetic resonance spectroscopy and theoretical calculations. *J. Med. Chem.* **1999**, *42*, 1714—1722.

(10) Zoumpoulakis, P.; Grdadolnik, S. G.; Matsoukas, J.; Mavromoustakos, T. Structure elucidation and conformational properties of eprosartan a non peptide angiotensin II AT_1 antagonist. *J. Pharm. Biomed. Anal.* **2002**, *28*, 125—135.

(11) Zoumpoulakis, P.; Zoga, A.; Roumelioti, P.; Giatas, N.; Grdadolnik, S. G.; Iliodromitis, E.; Vlahakos, D.; Kremastinos, D.; Matsoukas, J. M.; Mavromoustakos, T. Conformational and biological studies for a pair of novel synthetic AT_1 antagonists: stereoelectronic requirements for antihypertensive efficacy. *J. Pharm. Biomed. Anal.* **2003**, *31*, 833—844.

(12) Zoumpoulakis, P.; Politi, A.; Grdadolnik, S. G.; Matsoukas, J.; Mavromoustakos, T. Structure elucidation and conformational study of V8: A novel synthetic non peptide AT_1 antagonist. *J. Pharm. Biomed. Anal.* **2006**, *40*, 1097—1104.

(13) Zoumpoulakis, P.; Mavromoustakos, T. Seeking the active site of the AT_1 receptor for computational docking studies. *Drug Des. Rev.* **2005**, *2*, 537—545.

(14) Zoumpoulakis, P.; Daliani, I.; Zervou, M.; Kyrikou, I.; Siapi, E.; Lamprinidis, G.; Mikros, E.; Mavromoustakos, T. Losartan's molecular basis of interaction with membranes and AT$_1$ receptor. *Chem. Phys. Lipids.* **2003**, *125*, 13−25.

(15) Matsoukas, M.-T.; Zoumpoulakis, P.; Tselios, T. Conformational analysis of aliskiren, a potent renin inhibitor, using high-resolution nuclear magnetic resonance and molecular dynamics simulations. *J. Chem. Inf. Model.* **2011**, *51*, 2386−2397.

(16) Matsoukas, J. M.; Scanlon, M. N.; Moore, G. J. A cyclic angiotensin antagonist: [1,8-cysteine]angiotensin II. *J. Med. Chem.* **1984**, *27*, 404−406.

(17) Matsoukas, J. M.; Moore, G. J. NMR studies on angiotensin II: Histidine and phenylalanine ring stacking and biological activity. *Biochem. Biophys. Res. Commun.* **1984**, *122*, 434−438.

(18) Matsoukas, J.; Cordopatis, P.; Belte, U.; Goghari, M. H.; Ganter, R. C.; Franklin, K. J.; Moore, G. J. Importance of the N-terminal domain of the type II angiotensin antagonist sarmesin for receptor blockade. *J. Med. Chem.* **1988**, *31*, 1418−1421.

(19) Matsoukas, J. M.; Moore, G. J. NMR and mass spectroscopic studies of the competitive-angiotensin II antagonist "sarmesin". *Spectrosc. Lett.* **1988**, *21*, 477−491.

(20) Matsoukas, J. M.; Hondrelis, J.; Keramida, M.; Mavromoustakos, T.; Makriyannis, A.; Yamdagni, R.; Wu, Q.; Moore, G. J. Role of the NH$_2$-terminal domain of angiotensin II (ANG II) and [Sar^1]angiotensin II on conformation and activity. *J. Biol. Chem.* **1994**, *269*, 5303−5312.

(21) Matsoukas, J. M.; Polevaya, L.; Ancans, J.; Mavromoustakos, T.; Kolocouris, A.; Roumelioti, P.; Vlahakos, D. V.; Yamdagni, R.; Wu, Q.; Moore, G. J. The design and synthesis of a potent angiotensin II cyclic analogue confirms the ring cluster receptor conformation of the hormone angiotensin II. *Bioorg. Med. Chem.* **2000**, *8*, 1−10.

(22) Matsoukas, J. M.; Goghari, M. H.; Moore, G. J. Proton magnetic resonance studies of angiotensin II conformation: chemical shifts for the aromatic protons of selected analogues in DMSO-d6 at 400 Mz. In *Peptides 1986*, Walter de Gruyter & Co: Berlin, 1987; pp 335−339.

(23) Moore, G. J.; Matsoukas, J. M. Angiotensin as a model for hormone - receptor interactions. *Biosci. Rep.* **1985**, *5*, 407−416.

(24) Tzakos, A. G.; Bonvin, A. M. J. J.; Troganis, A.; Cordopatis, P.; Amzel, M. L.; Gerothanassis, I. P.; van Nuland, N. A. J. On the molecular basis of the recognition of angiotensin II (AII). *Eur. J. Biochem.* **2003**, *270*, 849−860.

(25) Taddese, B.; Simpson, L. M.; Wall, I. D.; Blaney, F. E.; Reynolds, C. A. Modeling Active GPCR Conformations. In *Methods in Enzymology*, Conn, P. M., Ed.; Academic Press: 2013; Vol. *522*, pp 21−35.

(26) Harrison, C. G protein-coupled receptors: Homology model allows effective virtual screening. *Nat. Rev. Drug Discov.* **2011**, *10*, 816−816.

(27) Fredriksson, R.; Lagerstrom, M. C.; Lundin, L.-G.; Schioth, H. B. The G-protein-coupled receptors in the human genome form five main families. Phylogenetic analysis, paralogon groups, and fingerprints. *Mol. Pharmacol.* **2003**, *63*, 1256−1272.

(28) Wu, B.; Chien, E. Y. T.; Mol, C. D.; Fenalti, G.; Liu, W.; Katritch, V.; Abagyan, R.; Brooun, A.; Wells, P.; Bi, F. C.; Hamel, D. J.; Kuhn, P.; Handel, T. M.; Cherezov, V.; Stevens, R. C. Structures of the CXCR4 chemokine GPCR with small-molecule and cyclic peptide antagonists. *Science* **2010**, *330*, 1066−1071.

(29) Takezako, T.; Gogonea, C.; Saad, Y.; Noda, K.; Karnik, S. S. "Network leaning" as a mechanism of insurmountable antagonism of the angiotensin II type 1 receptor by non-peptide antagonists. *J. Biol. Chem.* **2004**, *279*, 15248−15257.

(30) Yan, L.; Holleran, B. J.; Lavigne, P.; Escher, E.; Guillemette, G.; Leduc, R. Analysis of transmembrane domains 1 and 4 of the human angiotensin II AT$_1$ receptor by cysteine-scanning mutagenesis. *J. Biol. Chem.* **2010**, *285*, 2284−2293.

(31) Yamano, Y.; Ohyama, K.; Kikyo, M.; Sano, T.; Nakagomi, Y.; Inoue, Y.; Nakamura, N.; Morishima, I.; Guo, D.-F.; Hamakubo, T.; Inagami, T. Mutagenesis and the molecular modeling of the rat angiotensin II receptor. *J. Biol. Chem.* **1995**, *270*, 14024−14030.

(32) Feng, Y.-H.; Noda, K.; Saad, Y.; Liu, X.; Husain, A.; Karnik, S. S. The docking of Arg^2 of angiotensin II with Asp^{281} of AT$_1$ receptor is essential for full agonism. *J. Biol. Chem.* **1995**, *270*, 12846−12850.

(33) Arsenault, J.; Cabana, J.; Fillion, D.; Leduc, R.; Guillemette, G.; Lavigne, P.; Escher, E. Temperature dependent photolabeling of the human angiotensin II type 1 receptor reveals insights into its conformational landscape and its activation mechanism. *Biochem. Pharmacol.* **2010**, *80*, 990−999.

(34) Ballesteros, J. A.; Weinstein, H. Integrated methods for the construction of three-dimensional models and computational probing of structure-function relations in G protein-coupled receptors. In *Methods in Neurosciences*, Stuart, C. S., Ed.; Academic Press: 1995; Vol. *25*, pp 366−428.

(35) Noda, K.; Saad, Y.; Kinoshita, A.; Boyle, T. P.; Graham, R. M.; Husain, A.; Karnik, S. S. Tetrazole and carboxylate groups of angiotensin receptor antagonists bind to the same subsite by different mechanisms. *J. Biol. Chem.* **1995**, *270*, 2284−2289.

(36) Hansson, T.; Marelius, J.; Aqvist, J. Ligand binding affinity prediction by linear interaction energy methods. *J. Comput-Aided. Mol. Des.* **1998**, *12*, 27−35.

(37) Martin, S. S.; Holleran, B. J.; Escher, E.; Guillemette, G.; Leduc, R. Activation of the angiotensin II type 1 receptor leads to movement of the sixth transmembrane domain: Analysis by the substituted cysteine accessibility method. *Mol. Pharmacol.* **2007**, *72*, 182−190.

(38) Fillion, D.; Cabana, J.; Guillemette, G.; Leduc, R.; Lavigne, P.; Escher, E. Structure of the human angiotensin II type 1 (AT$_1$) receptor bound to angiotensin II from multiple chemoselective photoprobe contacts reveals a unique peptide binding mode. *J. Biol. Chem.* **2013**, *288*, 8187−8197.

(39) Eswar, N.; Webb, B.; Marti-Renom, M. A.; Madhusudhan, M. S.; Eramian, D.; Shen, M.-y.; Pieper, U.; Sali, A. Comparative protein structure modeling using Modeller. In *Current Protocols in Bioinformatics*, John Wiley & Sons, Inc.: 2002.

(40) Boucard, A. A. Constitutive activation of the angiotensin II type 1 receptor alters the spatial proximity of transmembrane 7 to the ligand-binding pocket. *J. Biol. Chem.* **2003**, *278*, 36628−36636.

(41) Bockenhauer, S.; Furstenberg, A.; Yao, X. J.; Kobilka, B. K.; Moerner, W. E. Conformational dynamics of single G protein-coupled receptors in solution. *J. Phys. Chem. B* **2011**, *115*, 13328−13338.

(42) Nygaard, R.; Zou, Y.; Dror, R. O.; Mildorf, T. J.; Arlow, D. H.; Manglik, A.; Pan, A. C.; Liu, C. W.; Fung, J. J.; Bokoch, M. P.; Thian, F. S.; Kobilka, T. S.; Shaw, D. E.; Mueller, L.; Prosser, R. S.; Kobilka, B. K. The dynamic process of β_2-adrenergic receptor activation. *Cell* **2013**, *152*, 532−542.

(43) Rasmussen, S. G. F.; Choi, H. J.; Rosenbaum, D. M.; Kobilka, T. S.; Thian, F. S.; Edwards, P. C.; Burghammer, M.; Ratnala, V. R. P.; Sanishvili, R.; Fischetti, R. F.; Schertler, G. F. X.; Weis, W. I.; Kobilka, B. K. Crystal structure of the human β_2 adrenergic G-protein-coupled receptor. *Nature* **2007**, *450*, 383−388.

(44) Han, D. S.; Wang, S. X.; Weinstein, H. Active state-like conformational elements in the β_2-AR and a photoactivated intermediate of rhodopsin identified by dynamic properties of GPCRs. *Biochemistry* **2008**, *47*, 7317−7321.

(45) Cabana, J.; Holleran, B.; Beaulieu, M.-E.; Leduc, R.; Escher, E.; Guillemette, G.; Lavigne, P. Critical hydrogen bond formation for activation of the angiotensin II type 1 receptor. *J. Biol. Chem.* **2013**, *288*, 2593−2604.

(46) Griesinger, C.; Ernst, R. R. Frequency offset effects and their elimination in NMR rotating-frame cross-relaxation spectroscopy. *J. Magn. Reson.* **1987**, *75*, 261−271.

(47) *MacroModel*, version 9.9; Schrodinger, LLC: New York, NY, 2012.

(48) The UniProt Consortium. Reorganizing the protein space at the Universal Protein Resource (UniProt). *Nucleic Acids Res.* **2012**, *40*, D71−D75.

(49) Li, J.; Edwards, P.; Burghammer, M.; Villa, C.; Schertler, G. Structure of bovine rhodopsin in a trigonal crystal form. *J. Mol. Biol.* **2004**, *343*, 1409−1438.

(50) Shen, M.-Y.; Sali, A. Statistical potential for assessment and prediction of protein structures. *Protein Sci.* **2006**, *15*, 2507−2524.

(51) Laskowski, R. A.; MacArthur, M. W.; Moss, D. S.; Thornton, J. M. PROCHECK: a program to check the stereochemical quality of protein structures. *J. Appl. Crystallogr.* **1993**, *26*, 283−291.

(52) *Glide, Induced Fit Docking protocol*, version 5.8; Schrodinger, LLC: New York, NY, 2012.

(53) Nirula, V.; Zheng, W.; Sothinathan, R.; Sandberg, K. Interaction of biphenylimidazole and imidazoleacrylic acid nonpeptide antagonists with valine 108 in TM III of the AT_1 angiotensin receptor. *Br. J. Pharmacol.* **1996**, *119*, 1505−1507.

(54) Corrêa, S. A. A.; Pignatari, G. C.; Ferro, E. S.; Pacheco, N. A. S.; Costa-Neto, C. M.; Pesquero, J. B.; Oliveira, L.; Paiva, A. C. M.; Shimuta, S. I. Role of the Cys^{18}−Cys^{274} disulfide bond and of the third extracellular loop in the constitutive activation and internalization of angiotensin II type 1 receptor. *Regul. Pept.* **2006**, *134*, 132−140.

(55) Ohno, K.; Amano, Y.; Kakuta, H.; Niimi, T.; Takakura, S.; Orita, M.; Miyata, K.; Sakashita, H.; Takeuchi, M.; Komuro, I.; Higaki, J.; Horiuchi, M.; Kim-Mitsuyama, S.; Mori, Y.; Morishita, R.; Yamagishi, S.-i. Unique "delta lock" structure of telmisartan is involved in its strongest binding affinity to angiotensin II type 1 receptor. *Biochem. Biophys. Res. Commun.* **2011**, *404*, 434−437.

(56) Miura, S.-I.; Fujino, M.; Hanzawa, H.; Kiya, Y.; Imaizumi, S.; Matsuo, Y.; Tomita, S.; Uehara, Y.; Karnik, S. S.; Yanagisawa, H.; Koike, H.; Komuro, I.; Saku, K. Molecular mechanism underlying inverse agonist of angiotensin II type 1 receptor. *J. Biol. Chem.* **2006**, *281*, 19288−19295.

(57) Fiser, A.; Do, R. K. G.; Šali, A. Modeling of loops in protein structures. *Protein Sci.* **2000**, *9*, 1753−1773.

(58) Berendsen, H. J. C.; van der Spoel, D.; van Drunen, R. GROMACS: A message-passing parallel molecular dynamics implementation. *Comput. Phys. Commun.* **1995**, *91*, 43−56.

(59) Cordomí, A.; Edholm, O.; Perez, J. J. Effect of different treatments of long-range interactions and sampling conditions in molecular dynamic simulations of rhodopsin embedded in a dipalmitoyl phosphatidylcholine bilayer. *J. Comput. Chem.* **2007**, *28*, 1017−1030.

(60) Lindorff-Larsen, K.; Piana, S.; Palmo, K.; Maragakis, P.; Klepeis, J. L.; Dror, R. O.; Shaw, D. E. Improved side-chain torsion potentials for the Amber ff99SB protein force field. *Proteins: Struct. Funct. Bioinf.* **2010**, *78*, 1950−1958.

(61) Berger, O.; Edholm, O.; Jähnig, F. Molecular dynamics simulations of a fluid bilayer of dipalmitoylphosphatidylcholine at full hydration, constant pressure, and constant temperature. *Biophys. J.* **1997**, *72*, 2002−2013.

(62) Cordomi, A.; Caltabiano, G.; Pardo, L. Membrane protein simulations using AMBER force field and Berger lipid parameters. *J. Chem. Theory Comput.* **2012**, *8*, 948−958.

(63) Miyamoto, S.; Kollman, P. A. Settle: An analytical version of the SHAKE and RATTLE algorithm for rigid water models. *J. Comput. Chem.* **1992**, *13*, 952−962.

(64) Darden, T.; York, D.; Pedersen, L. Particle mesh Ewald: An N log(N) method for Ewald sums in large systems. *J. Chem. Phys.* **1993**, *98*, 10089−10092.

(65) Almlöf, M.; Åqvist, J.; Smalås, A. O.; Brandsdal, B. O. Probing the effect of point mutations at protein-protein interfaces with free energy calculations. *Biophys. J.* **2006**, *90*, 433−442.